Final Project Report

Project Title: "Major improvements on the longwave radiative interactions between surface and clouds in the Polar Regions in atmospheric global circulation model (GCM)"

Sponsor Award No. DE-SC0013080

Texas A&M University Account No.: 02-442811

Program Manager: Dr. Dorothy M. Koch
Earth System Modeling, BER, DOE
Email address: Dorothy.Koch@science.doe.gov

Principal Investigator: Prof. Ping Yang
Department of Atmospheric Sciences
Texas A&M University College Station, TX 77843
Email address: pyang@tamu.edu

Funding Period: 01/15/2016 – 01/14/2018

Submission Date: 02/06/2018

1. Summary of Work and Accomplishments in Year 1 (01/15/2015-01/14/2016)

We developed new ice cloud parameterizations based on state-of-the-art MODIS Collection 6 (MC6) ice particle model. Features of the model include the consideration of surface roughness of ice crystals and spectral consistency in cloud property retrievals. Using more than 14,000 particle size distributions (PSDs) from in-situ measurements and the latest ice particle single-scattering property library, our parameterizations provide band-averaged bulk-scattering properties. According to statistics of fittings, the parameterization schemes represent the band-averaged bulk-scattering properties very well. Compared to the ice particle model developed by Fu (1998), flux simulations with the MC6 particle model result in larger upward flux at the top of the atmosphere (TOA) and smaller at the surface for typical cirrus clouds. In the assessment of the effect of longwave light scattering, our results also support the conclusions of previous studies. The error in flux calculations reaches about 10 W/m^2 when a cirrus cloud is thin and its particle size is small.

2. Summary of Work and Accomplishments in Year 2 (01/15/2016-01/14/2017)

Clouds are a major modulator of the global radiation budgets. However, representations of clouds in general circulation models (GCMs) neglect many important processes, particularly those related to ice clouds. One major uncertainty source is the radiative transfer scheme in GCMs. To reduce the computational burden in most GCMs, absorption is the only radiative transfer process considered in longwave spectral bands. Recently, a state-of-the-art MC6 ice model has been available, which provides spectral consistency in ice cloud retrievals. With an advanced light scattering library for ice particles, we performed sensitivity studies of the potential impacts on the climate including light scattering for MC6 model and other 11 ice cloud models. Specifically, we modified RRTMG_LW (the GCM version of Longwave Rapid Radiative Transfer Model), a radiative transfer module widely used in GCMs and numerical prediction models, to identify flux simulation differences with and without considering light scattering processes. The simulations with light scattering come from a rigorous radiative solver, DISORT (Discrete Ordinates Radiative Transfer Program for a Multi-Layered Plane-Parallel Medium), are used as benchmarks. The results show that the weighted annual mean biases of RRTMG_LW for the upward flux at the top of the atmosphere, the downward flux at the surface, and the net flux into the atmosphere are about 0.8 ± 0.3, -0.1 ± 0.05, and -0.7 ± 0.3 W m-2, respectively. According to the different the ice crystal shapes, the weighted annual mean bias for heating rate is about -0.006 ± 0.02 to 0.04 K/day.

3. Summary of Work and Accomplishments in Year 3 (01/15/2017-01/14/2018)

Since absorption dominates optical properties of clouds in the longwave (LW) spectrum, most of general circulation models (GCMs) only take absorption properties of clouds into account in the radiative transfer modules in order to reduce computational costs. To quantify the biases of excluding LW scattering when clouds exist, we simulated fluxes and heating rates by using satellite data from Cloud-Aerosol Lidar and Infrared Pathfinder Satellite Observation (CALIPSO), CloudSat, Clouds and the Earth's Radiant Energy System (CERES) and Moderate Resolution Imaging Spectrometer (MODIS) merged products (CCCM) in 2010. In annual global average, neglecting LW scattering causes overestimation by 2.6 W/m^2 for the top-of-atmosphere (TOA) upward fluxes and underestimation by 1.2 W/m^2 for surface downward fluxes. In particular, regional extreme biases are approximately 12 W/m^2 for TOA upward fluxes and are approximately -3.6 W/m^2 for surface downward fluxes, or are approximately 5% of the global averaged outgoing longwave radiation (OLR) and 1% of the global averaged surface downward fluxes, respectively. In terms of heating rates, on average, LW scattering heats the whole atmosphere column by 0.0045 K/day, heats the cloud layers by 0.0420 K/day, heats the surface by 0.028 K/day, and cools the tropopause by 0.018 K/day.

4. Conference Presentations and Peer-reviewed Publications

Based on the outcomes of our research effort, our Texas A&M (TAMU) team leads a peer-reviewed paper in the *Journal of Advances in Modeling Earth Systems*. In addition, our TAMU team also contributed to two papers (one led by the collaborators at DOE Lawrence Berkeley National Laboratory, and one led by our collaborators at the University of Michigan). Our TAMU team also gave a number of presentations at national and international conferences.

Journal Publication:

- Kuo, C.-P., P. Yang, X.L. Huang, D. Feldman, M. Flanner, C. Kuo and E. J. Mlawer (2017). Impact of multiple scattering on longwave radiative transfer involving clouds. *Journal of Advances in Modeling Earth Systems*, 9(8), 3082–3098. doi:10.1002/2017MS001117.
- Kuo, C., Feldman, D. R., Huang, X., Flanner, M., Yang, P., & Chen, X. (2018). Time-dependent cryospheric longwave surface emissivity feedback in the Community Earth System Model. *Journal of Geophysical Research: Atmospheres*, 123. https://doi.org/10.1002/2017JD027595

- Huang, X., X. Chen, M. Flanner, P. Yang, D. Feldman, and C. Kuo, Improved representations of surface spectral emissivities in a global climate and its impact on the simulated climate. *Journal of Climate* (in review)

Conference Presentations led by our TAMU team:

- Kuo, C.-P., P. Yang, X.L. Huang, D. Feldman, and M. Flanner: Impact of multiple scattering on infrared radiative transfer involving ice clouds, AGU Annual Meeting, 12/14/2015-12/18/2015, San Francisco, CA, USA.
- Gu, B., P. Yang, K. P. Bowman, and P. Minnis: Comparison between RRTM and LBLRTM-DISORT for radiative transfer in scattering atmospheres, AGU Annual Meeting, 12/14/2015-12/18/2015, San Francisco, CA, USA.
- Kuo, C.-P., P. Yang, X.L. Huang, D. Feldman, and M. Flanner: Evaluation of light scattering by ice clouds in the infrared spectrum, AOGS Annual Meeting, 7/31/2016-8/5/2016, Beijing, China.
- Kuo, C.-P., P. Yang, X.L. Huang, D. Feldman, and M. Flanner: The impacts of light scattering by clouds on longwave radiative transfer, AGU Annual Meeting, 12/12/2016-12/16/2016, San Francisco, CA.
- Kuo, C.-P., P. Yang, X.L. Huang, D. Feldman, M. Flanner, C. Kuo and E. J. Mlawer: The potential influence of multiple scattering on longwave flux and heating rate simulations with clouds, AGU Annual Meeting, 12/11/2017-12/15/2017, New Orleans, LA.
- Kuo, C.-P., P. Yang, X.L. Huang, D. Feldman, M. Flanner, C. Kuo and E. J. Mlawer: Toward accurate, efficient, and consistent global flux simulations, AMS Annual Meeting, 1/7/2018-1/11/2018, Austin, TX.

5. Teleconferences

ACME-teleconference	Date	Speaker	Contents
2nd time	05/23/2015	Dr. Ping Yang	Single-scattering properties of ice crystal and techniques to obtain these properties
2nd time	05/23/2015	Chia-Pang Kuo	Scattering effect of ice cloud
3rd time	06/20/2015	Chia-Pang Kuo	Parameterizations of MODIS collection-6 ice particle model
6th time	07/22/2016	Chia-Pang Kuo	Spatial, temporal and spectral analysis of longwave light scattering with different habits of ice clouds

6. Highlights of Year-3 Research

6.1. Science Background

Model approximations of radiative processes cause uncertainties in climate simulations. In the LW spectral bands, fluxes are usually calculated by approximations that assume only absorption because cloud absorption dominates scattering,. However, some studies find significant influences of scattering in LW radiative transfer. Ritter and Geleyn (1992) report a 16.2 W/m^2 decrease in OLR when considering scattering from a cloud between 12 and 13 km altitude with liquid water content of 0.01 g/m^2. Edwards and Slingo (1996) show the importance of scattering as a function of ice water path. Stephens et al. (2001) estimate that the global mean OLR decreases by 8 W/m^2 in global climate model simulations when contributions from scattering are included. Using surface observations, Joseph and Min (2003) suggest that OLR is overestimated by as much as 6-8 W/m^2 due to neglecting LW scattering by thin cirrus clouds. Costa and Shine (2006) estimate a 3 W/m^2 reduction in OLR from 60°S to 60°N due to light scattering in models considering hexagonal ice particles and spherical liquid droplets. Schmidt et al. (2006) state that LW scattering decreases OLR by about 1.5 W/m^2 and increase surface downward flux by about 0.4 W/m^2.

According to those studies, estimates of the influence of LW light scattering by clouds on OLR vary by approximately one order of magnitude when clouds are present. In order to give an evaluation of climate effects based on the current level of understanding of cloud radiative properties, we characterize the uncertainties of flux and heating rate simulations by using rigorous radiative transfer calculations combined with satellite observations.

6.2. Cloud Optical Models

The cloud optical models used in this study are so-called MODIS Collection 6 (MC6) cloud models (Platnick et al., 2015; Platnick et al., 2017), which contain ice and water clouds. The MC6 ice cloud model assumes an aggregate of 8 severely roughened columns for ice cloud crystals. The optical properties of ice crystals are provided by Yang's ice crystal library (Yang et al., 2013), which uses refractive index of ice from Warren and Brandt (2008). For the MC6 water cloud model, which assumes spheres for water cloud droplets, the optical properties are computed by the Lorenz-Mie theory (van de Hulst, 1957; Bohren and Huffman, 1998) with the refractive index of water from compilations by Hale and Querry (1973) (0.25 μm < wavelength < 0.69 μm), Palmer and Williams (1974) (0.69 μm < wavelength < 2.0 μm), and Downing and Williams (1975) (wavelength > 2.0 μm).

6.3. Radiative Transfer Model Settings

In order to estimate flux and heating rate biases due to neglecting LW scattering of clouds, since the radiative transfer module in the GCM version of the Longwave Rapid Radiative Transfer Model (RRTMG_LW) (Clough et al., 2005; Iacono et al., 2008) only considers absorption processes, the rigorous radiative solver, Discrete Ordinates Radiative Transfer Program for a Multi-Layered Plane-Parallel Medium (DISORT) (Stamnes et al., 1988), is manually implemented into RRTMG_LW and the combined model is called RRTMG_LW/DISORT in this study. The simulation biases are defined as results calculated by absorption approximation minus results calculated by rigorous radiative transfer. In the both absorption approximation and rigorous calculation runs, we use the same RRTMG_LW/DISORT to simulate fluxes and heating rates to make simulations consistent. To properly deal with absorption approximation in RRTMG_LW/DISORT, we set single-scattering albedo to zero and use absorption optical thickness of the cloud to eliminate the influence of scattering. On the other hand, extinction optical thickness and single-scattering albedo are used in the rigorous radiative transfer simulations.

6.4. Satellite Observations

In our simulations, the Information about clouds and the atmosphere comes from Cloud-Aerosol Lidar and Infrared Pathfinder Satellite Observation (CALIPSO), CloudSat, Clouds and the Earth's Radiant Energy System (CERES) and Moderate Resolution Imaging Spectrometer (MODIS) merged products (CCCM Edition B1; Kato et al., 2010, 2011, 2014) in 2010. From the products, cloud microphysical and optical properties, including cloud phase, cloud optical thickness, cloud effective diameter, cloud fraction, and cloud top and base heights, are used in simulations. For atmospheric states, we not only use temperature, water vapor, and ozone profiles from the products, but also set concentrations of carbon dioxide (CO_2), nitrous oxide (N_2O), and methane (CH_4) to 390.5, 0.3242, and 1.803 ppmv, respectively, from the Fifth Assessment Report of the Intergovernmental Panel on Climate Change (IPCC, 2014).

6.5. Results and Discussions

Figure 1a shows spatial distributions of upward flux biases at the TOA when the LW scattering is neglected. Upward flux biases at the TOA along the Intertropical Convergence Zone (ITCZ) and in the Tibetan Plateau region are relatively larger than other areas, since ice clouds are profound over these regions. The local maximum biases are up to 12 W/m^2, which is about 5% of global average OLR (233.8

W/m^2; Henderson et al., 2013). However, in Figure 1b, since water vapor absorbs most of the downward scattered fluxes, the signal of downward flux biases at the surface is weaker in the tropics. Therefore, downward flux at the surface is significantly underestimated in the dry and high altitude regions, like Tibetan Plateau, the Antarctic, and Greenland. The regional peak biases are about 3.6 W/m^2, which is approximately 1% of global average surface downward flux (351.9 W/m^2; Henderson et al., 2013).

One-year global average flux biases for total clouds, ice clouds, and water clouds are present in Figure 2a. For ice clouds, global annual averaged biases of upward flux at the TOA and at the tropopause, and downward flux at the surface and at the tropopause are approximately 4.38, 4.39, -1.27, and -0.24 W/m^2, respectively. Furthermore, for water clouds, global annual averaged upward flux biases at the TOA and at the tropopause are about 1.55 and 1.62 W/m^2, respectively, and downward flux biases at the surface and at the tropopause are about -1.08 and -0.004 W/m^2, respectively. In general, the absolute flux biases are larger for ice clouds than for water clouds, because ice clouds have stronger single-scattering properties. The magnitude of biases is larger at the TOA than at the surface, since most of the downward scattered fluxes are absorbed by the water vapor without reaching the surface. Overall, excluding LW scattering in flux simulations causes overestimations of upward flux at the TOA by 2.63 W/m^2 and at the tropopause by 2.68 W/m^2, and underestimations of downward flux at the surface by 1.15 W/m^2 and at the tropopause by 0.09 W/m^2. As a result, about 1.48 W/m^2 is accumulated in the atmosphere when LW scattering is considered in the simulations.

Figure 2b describes global average biases for total clouds, ice clouds, and water clouds. Without consideration of LW scattering in simulations, heating rate biases for column mean, cloud layer mean, above cloud layer mean, under cloud layer mean, tropopause, and surface heating rates for ice clouds are about -0.0104, -0.0335, 0.0075, -0.0406, 0.0444, and -0.0262 K/day, respectively, and are about -0.0008, -0.0473, 0.0051, -0.0298, 0.0021, and -0.0294 K/day, respectively, for water clouds. Consequently, heating rate biases for total clouds are -0.0045, -0.0420, 0.0060, -0.0340, 0.0183, and -0.0282 K/day, respectively, for column mean, cloud layer mean, above cloud layer mean, under cloud layer mean, tropopause, and surface heating rates. The absolute column mean heating rate biases are quite small due to cancellation of positive and negative biases, but heating rate biases are non-negligible for cloud layer mean, above cloud layer mean, under cloud layer mean, tropopause, and surface.

6.6. Conclusions

Since most of the GCMs only consider absorption but not scattering properties of clouds in the LW spectrum to mitigate computational cost, in the study, flux and heating rate biases due to neglecting

LW scattering are quantified by using cloud and atmosphere information from CCCM products. One year global simulations in 2010 show that upward flux biases at the TOA are considerable in the ITCZ and in the Tibetan Plateau region, and the area containing significantly downward flux biases at the surface are in the dry and high altitude regions. Local extreme value for upward flux biases is at most 12 W/m^2, and for downward flux biases is about 3.6 W/m^2, which is about 5% of global average OLR (233.8 W/m^2) and 1 % of global average surface downward flux (351.9 W/m^2), respectively.

Averaging one year of global simulation flux biases, upward flux biases at the TOA are 2.63 W/m^2, and downward flux biases at the surface are -1.15 W/m^2, leading to 1.48 W/m^2 increase in the atmosphere. The intensity of biases is larger for upward flux at the TOA than for downward flux at the surface, since upper atmosphere is more transparent than lower atmosphere. For heating rates, while absolute column mean biases, about 0.0045 K/day, are small, biases for cloud layer mean are the largest and the magnitude is about 0.0420 K/day. In addition, LW scattering cools the tropopause approximately 0.0183 K/day and heats the surface about 0.0282 K/day. For different thermodynamic phases of clouds, simulation biases are larger for ice clouds than for water clouds in general.

7. Reference

Bohren, C. F., & Huffman, D. R. (1998). *Absorption and Scattering of Light by Small Particles*. New York: Wiley. doi:10.1002/9783527618156

Clough, S. A., Shephard, M. W., Mlawer, E. J., Delamere, J. S., Iacono, M. J., Cady-Pereira, K., … Brown, P. D. (2005). Atmospheric radiative transfer modeling: A summary of the AER codes. *Journal of Quantitative Spectroscopy and Radiative Transfer*, *91*(2), 233–244. doi:10.1016/j.jqsrt.2004.05.058

Costa, S. M. S., & Shine, K. P. (2006). An estimate of the global impact of multiple scattering by clouds on outgoing long-wave radiation. *Quarterly Journal of the Royal Meteorological Society*, *132*(616), 885–895. doi:10.1256/qj.05.169

Downing, H. D., & Williams, D. (1975). Optical constants of water in the infrared. *Journal of Geophysical Research*, *80*(12), 1656–1661. doi:10.1029/JC080i012p01656

Edwards, J. M., & Slingo, A. (1996). Studies with a flexible new radiation code. I: Choosing a configuration for a large-scale model. *Quarterly Journal of the Royal Meteorological Society*, *122*(531), 689–719. doi:10.1002/qj.49712253107

Fu, Q., Yang, P., & Sun, W. B. (1998). An accurate parameterization of the infrared radiative properties of cirrus clouds for climate models. *Journal of Climate*, *11*(9), 2223–2237. doi:10.1175/1520-0442(1998)011<2223:AAPOTI>2.0.CO;2

Hale, G. M., & Querry, M. R. (1973). Optical constants of water in the 200-nm to 200-μm wavelength region. *Applied Optics*, *12*(3), 555–563. doi:10.1364/AO.12.000555

Henderson, D. S., L'Ecuyer, T., Stephens, G., Partain, P., & Sekiguchi, M. (2013). A multisensor perspective on the radiative impacts of clouds and aerosols. *Journal of Applied Meteorology and Climatology*, *52*(4), 853–871. doi:10.1175/JAMC-D-12-025.1

Iacono, M. J., Delamere, J. S., Mlawer, E. J., Shephard, M. W., Clough, S. A., & Collins, W. D. (2008). Radiative forcing by long-lived greenhouse gases: Calculations with the AER radiative transfer models. *Journal of Geophysical Research: Atmospheres*, *113*(13), 2–9. doi:10.1029/2008JD009944

IPCC (2014). *Climate Change 2013: The Physical Science Basis. Contribution of Working Group I to the Fifth Assessment Report of the Intergovernmental Panel on Climate Change*. (T. F. Stocker, D. Qin, G.-K. Plattner, M. Tignor, S. K. Allen, J. Boschung, … P. M. Midgley, Eds.). Cambridge, NY: Cambridge University Press. doi:10.1017/CBO9781107415324

Joseph, E., & Min, Q. (2003). Assessment of multiple scattering and horizontal inhomogeneity in IR radiative transfer calculations of observed thin cirrus clouds. *Journal of Geophysical Research: Atmospheres*, *108*(D13), 4380. doi:10.1029/2002JD002831

Kato, S., Sun-Mack, S., Miller, W. F., Rose, F. G., Chen, Y., Minnis, P., & Wielicki, B. A. (2010). Relationships among cloud occurrence frequency, overlap, and effective thickness derived from CALIPSO and CloudSat merged cloud vertical profiles. *Journal of Geophysical Research*, *115*(D4), D00H28. doi:10.1029/2009JD012277

Kato, S., Rose, F. G., Sun-Mack, S., Miller, W. F., Chen, Y., Rutan, D. A., … Collins, W. D. (2011). Improvements of top-of-atmosphere and surface irradiance computations with CALIPSO-, CloudSat-, and MODIS-derived cloud and aerosol properties. *Journal of Geophysical Research*, *116*(D19), D19209. doi:10.1029/2011JD016050

Kato, S., Miller, W. F., Sun-Mack, S., Rose, F. G., Chen, Y., & Mlynczak, P. E. (2014). Variable descriptions of the A-train integrated CALIPSO, CloudSat, CERES, and MODIS merged product (CCCM or C3M), Version RelB1.v2.

Kuo, C.-P., P. Yang, X.L. Huang, D. Feldman, M. Flanner, C. Kuo and E. J. Mlawer (2017). Impact of multiple scattering on longwave radiative transfer involving clouds. *Journal of Advances in Modeling Earth Systems*, 9(8), 3082–3098. doi:10.1002/2017MS001117.

Palmer, K. F., & Williams, D. (1974). Optical properties of water in the near infrared. *Journal of the Optical Society of America*, *64*(8), 1107–1110. doi:10.1364/JOSA.64.001107

Platnick, S., King, M. D., Meyer, K. G., Wind, G., Amarasinghe, N., Marchant, B., … Riedi, J. (2015). MODIS cloud optical properties: User guide for the Collection 6 Level-2 MOD06/MYD06 product and associated Level-3 Datasets, Version 1.0. Retrieved from http://modis-atmos.gsfc.nasa.gov/_docs/C6MOD06OPUserGuide.pdf

Platnick, S., Meyer, K. G., King, M. D., Wind, G., Amarasinghe, N., Marchant, B., … Riedi, J. (2017). The MODIS cloud optical and microphysical products: Collection 6 updates and examples from Terra and Aqua. *IEEE Transactions on Geoscience and Remote Sensing*, *55*(1), 502–525. doi:10.1109/TGRS.2016.2610522

Ritter, B., & Geleyn, J.-F. (1992). A comprehensive radiation scheme for numerical weather prediction models with potential applications in climate simulations. *Monthly Weather Review*, *120*(2), 303–325. doi:10.1175/1520-0493(1992)120<0303:ACRSFN>2.0.CO;2

Schmidt, G. A., Ruedy, R., Hansen, J. E., Aleinov, I., Bell, N., Bauer, M., … Yao, M.-S. (2006). Present-day atmospheric simulations using GISS ModelE: Comparison to in situ, satellite, and reanalysis data. *Journal of Climate*, *19*(2), 153–192. doi:10.1175/JCLI3612.1

Stamnes, K., Tsay, S.-C., Wiscombe, W., & Jayaweera, K. (1988). Numerically stable algorithm for discrete-ordinate-method radiative transfer in multiple scattering and emitting layered media. *Applied Optics*, *27*(12), 2502–2509. doi:10.1364/AO.27.002502

Stephens, G. L., Gabriel, P. M., & Partain, P. T. (2001). Parameterization of atmospheric radiative transfer. Part I: Validity of simple models. *Journal of the Atmospheric Sciences*, *58*(22), 3391–3409. doi:10.1175/1520-0469(2001)058<3391:POARTP>2.0.CO;2

van de Hulst, H. C. (1957). *Light Scattering by Small Particles*. New York: Wiley.

Warren, S. G., & Brandt, R. E. (2008). Optical constants of ice from the ultraviolet to the microwave: A revised compilation. *Journal of Geophysical Research: Atmospheres*, *113*(14), 1–10. doi:10.1029/2007JD009744

Yang, P., Bi, L., Baum, B. A., Liou, K.-N., Kattawar, G. W., Mishchenko, M. I., & Cole, B. (2013). Spectrally consistent scattering, absorption, and polarization properties of atmospheric ice crystals at wavelengths from 0.2 to 100 µm. *Journal of the Atmospheric Sciences*, *70*(1), 330–347. doi:10.1175/JAS-D-12-039.1

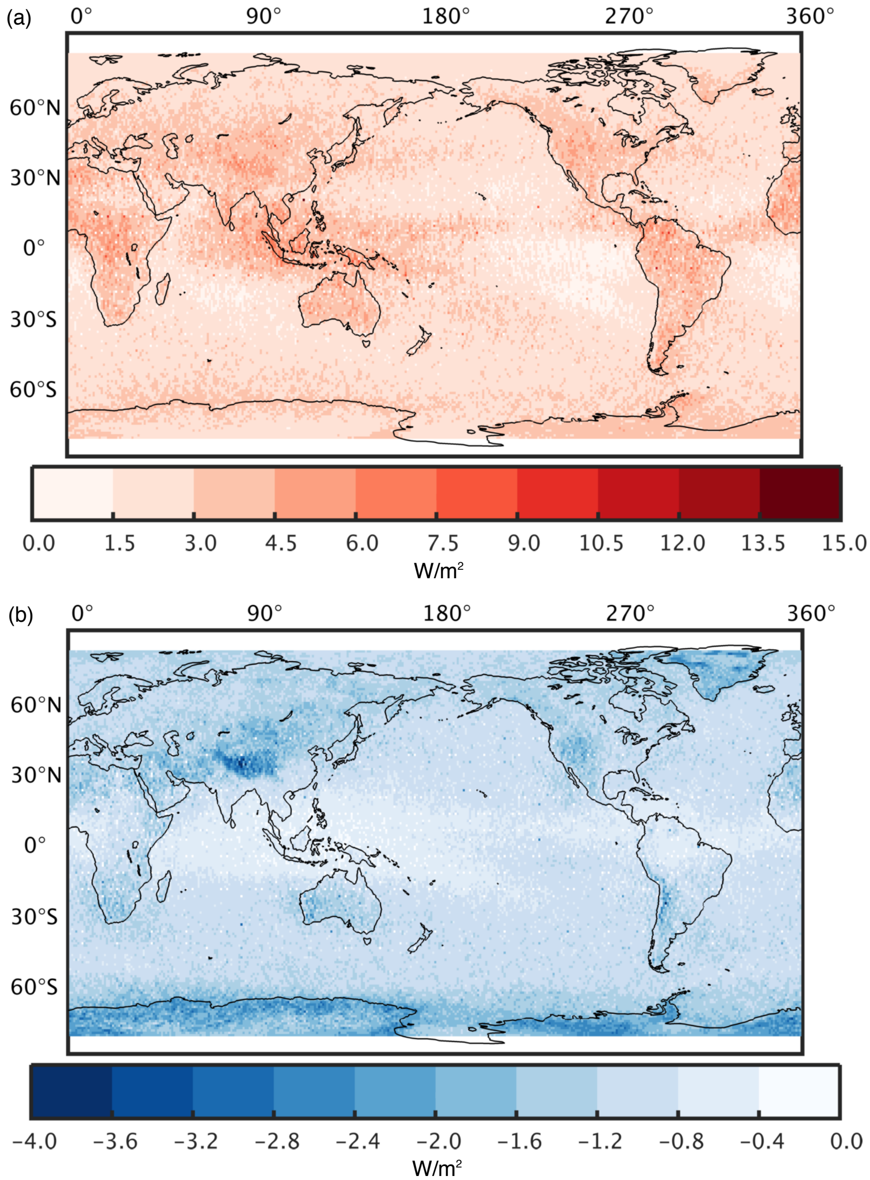

Figure 1. Global distributions (1° × 1°) of the annual mean biases in 2010 for (a) the upward flux at the TOA and (b) the downward flux at the surface. Blank regions indicate no satellite observations. Adapted from our publication by Kuo et al. (2017).

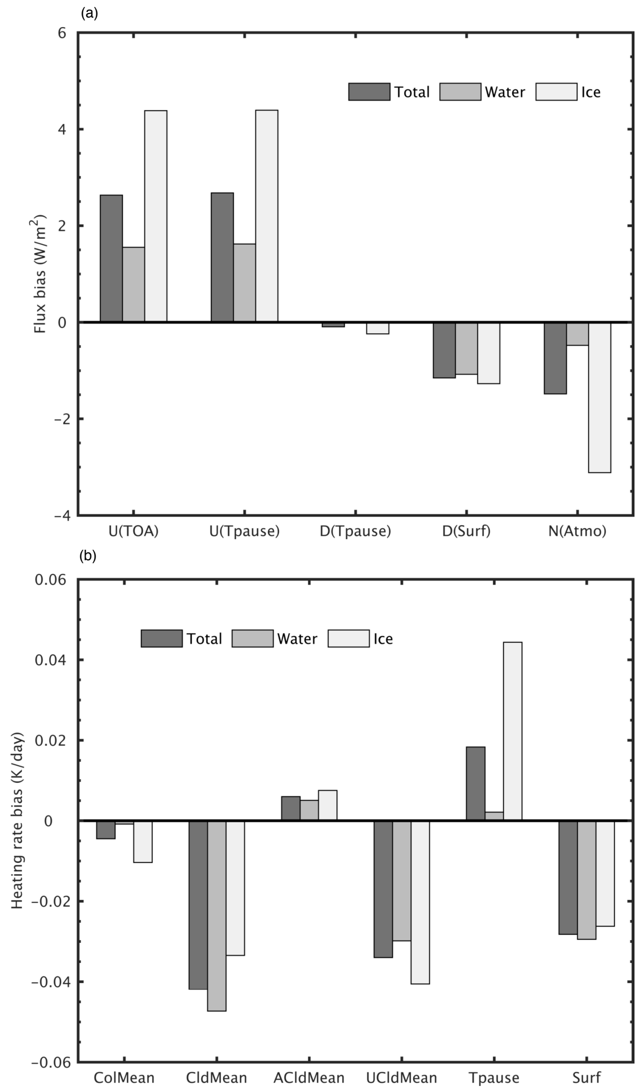

Figure 2. Annual global mean biases in 2010 of (a) the upward flux at the TOA [U(TOA)] and the tropopause [U(Tpause)], the downward flux at the surface [D(Surf)] and the tropopause [D(Tpause)], and the net flux into the atmosphere [N(Atmo)], and (b) the heating rate for ColMean, CldMean, UCldMean, ACldMean, Surf, and Tpause, which represent mean heating rate biases through the whole atmosphere column, in cloud layers, under cloud layers, above cloud layers, at the surface, and at the tropopause, respectively. “Total”, “water”, and “ice” mean total clouds, water clouds only, and ice clouds only, respectively. Adapted from our publication by Kuo et al. (2017).